Communication

A Cavity-Backed Annular Slot Antenna With High Efficiency for Smartwatches With Metallic Housing

Di Wu and S. W. Cheung

***Abstract*— A cavity-backed annular slot antenna designed for the use in smartwatches in the 2.4-GHz Wi-Fi band is proposed. The cavity is metallic and has a cylindrical shape with a volume of $\pi \times 21^2 \times 10$ mm^3. An annular slot is cut along the edge of the top surface (as the smartwatch screen) of the cavity. The circumference of the annular slot is about 1λ, making the design small enough for the smartwatch applications. The resonant modes, current distribution, and transverse mode of the cavity-backed annular slot antenna are studied using simulations and the results are used to design a smartwatch antenna. The proposed smartwatch is studied in free space, on a computer hand model, and on a phantom hand using simulations and measurements. Measured results show that the antenna has an efficiency of 57%–66% on a phantom hand. To study the antenna in a more realistic environment, the electronic components inside the smartwatch are modeled as a metallic block. For health risk concerns related to exposure to an electromagnetic radiation, the specific absorption rate for the smartwatch in the wrist-worn and next-to-mouth conditions is also studied using simulations.**

***Index Terms*— Annular slot antenna, cavity-backed antenna, high efficiency, metallic housing, smartwatch antenna, specific absorption rate (SAR).**

I. Introduction

Wearables are the electronic devices which you can "wear," such as smart watches, bracelets, glasses, and headsets [1]. Smartwatch, as one of the most favorite wearable devices, has gained increasing popularity in the consumer electronics market. By integrating sensors inside, smartwatch can be used to track the hydration level to inform when to drink water, track the activities using steps, distance, and calories, and know the location, and so on [2], [3]. The data recorded can be synchronized with other devices or systems. With the developments of low-power technologies and Internet of Things (IoT) [4], [5], smartwatch will be with more and wider applications in the future.

There are two major challenges in the design of antennas for smartwatches. The first challenge is the low antenna efficiency when the watch is worn on the human hand [1]. As human body has high loss for electromagnetic (EM) waves, part of the radiation energy from the antenna is absorbed by the human tissue and converted into heat, lowering down the antenna efficiency and leading to shorter battery life in the smartwatches. The second challenge is brought by the trend of using metallic housing for smartwatches due to recent fashions, i.e., to make smartwatches look like a jewelry [6]. Metallic housing can improve the rigidity and strength of thesmartwatches and build adorable metallic appearances for consumers, but metallic housing can also block wireless signals (Wi-Fi, Bluetooth, GPS, or other radio signals), making the antenna design difficult [6]. Therefore, the objective of this communication is to design an antenna which can achieve high antenna efficiency when applied in the smartwatches with metallic housing and worn on a human hand.

Manuscript received October 13, 2016; revised April 20, 2017; accepted May 12, 2017. Date of publication May 17, 2017; date of current version July 1, 2017. *(Corresponding author: Di Wu.)*

The authors are with the Department of Electrical and Electronic Engineering, The University of Hong Kong, Hong Kong (e-mail: diwu@eee.hku.hk; swcheung@eee.hku.hk).

Color versions of one or more of the figures in this communication are available online at http://ieeexplore.ieee.org.

Digital Object Identifier 10.1109/TAP.2017.2705223

TABLE I

Efficiencies of Antennas in [8]–[16] for Smartwatch

Ref.	Frequency band	Sim. efficiency in free space / on phantom hand	Mea. efficiency in free space / on phantom hand
[8]	MICS & 2.4 GHz Wi-Fi	99% / Not given	Not given
[9]	2.4 GHz Wi-Fi	80% / 30%*	Not given
[10]	0.7-2.7 GHz Cellular	Not given	80% average / 30% average**
[11]	2.4 GHz Wi-Fi	Not given / 5%	Not given
[12]	2.4 GHz Wi-Fi	69% / 26%	67-73% / Not given
[13]	GPS 2.4&5 GHz Wi-Fi	66.7% for 2.4G Wi-Fi / Not given	Not given
[14]	2.27-6.14 GHz	Not given	Not given
[15]	2.4 GHz Wi-Fi	Not given	70% average / Not given
[16]	2.4 GHz Wi-Fi	75-95% / 65-71%	Not given
Proposed	2.4 GHz Wi-Fi	81-97% / 67-83%	70-78% / 57-66%

* No upper ground plane

** Average efficiency from 1.7 to 2.2 GHz.

The different types of antennas can be used in the design of smartwatches, such as the inverted-F antennas in [7] and [8], monopoles in [9]–[11], loop antennas in [12] and [13], differential wideband metal-frame antenna in [14], and chip antenna in [15]. However, the efficiencies of these antennas, when worn on a phantom hand, dropped dramatically. Table I compares the efficiencies of these antennas, including our proposed antenna. It can be seen that when worn on a phantom hand, our proposed antenna has the highest efficiency. Furthermore, the antennas in [7]–[15] cannot be used in smartwatches with metallic housing, which blocks EM radiation and hence substantially degrades the performances, while the proposed antenna is designed on metallic housing and thus is not affected by metallic housing. Previously in [16], we used simulations to design a slot antenna for smartwatches on metallic housing with high efficiency (as shown in Table I) for the 2.4-GHz BT/Wi-Fi system. However, the antenna needs four shorting strips inside the cavity and two shorting strips on the top circular surface for matching, which makes the antenna very complicated and difficult to be fabricated.

As the backed metallic cavity can reduce backward radiation [17]–[19], a cavity-backed annular slot antenna can be well used to design smartwatch antennas to reduce energy absorption by human hand and hence to enhance the antenna efficiency. However, to the best of our knowledge, a cavity-backed annular slot antenna has never been studied for smartwatches with metallic housing. Thus, in this communication, we propose a cavity-backed annular slot antenna for

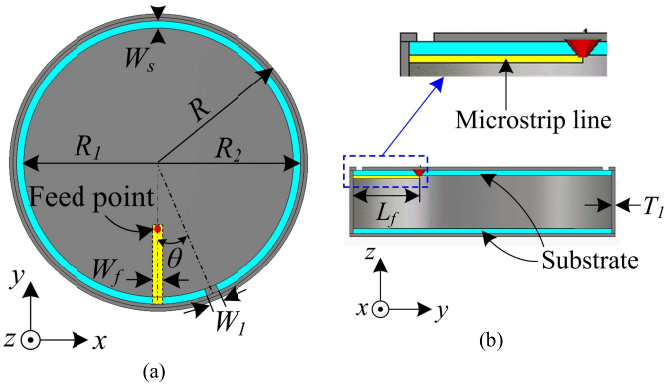

Fig. 1. Geometry of cavity-backed annular slot antenna (a) top view and (b) side view.

use in smartwatches with metallic housing for high efficiency in the 2.4-GHz Bluetooth/Wi-Fi band. In [19], the study showed that the required circumference of the annular slot on the cavity was about 1.5λ which, at 2.4 GHz, is too large for use in current smartwatches. Then, we propose to use an angle of 22.5° between the microstrip feed line and shorting strip on the annular slot so as to generate a lower resonant mode, the 1-λ mode, for the antenna. In the 1-λ mode, the required circumference for the annular slot can be reduced to about 1λ, only 2/3 of that used in [19], which, at 2.4 GHz, can well fit the size of current smartwatches. The proposed antenna in free space, on a computer hand model, and on a phantom hand is studied using the EM simulation tool CST and the antenna measurement equipment, the Satimo Starlab system [20]. The results show that when the smartwatch is worn on the phantom hand, the measured efficiency is about 57%–66%. The effects of metallic components inside the watch and specific absorption rate (SAR) are also analyzed.

II. Cavity-Backed Annular Slot Antenna for Smartwatches

The structure of the proposed cavity-backed annular slot antenna is shown in Fig. 1, which is similar to our previous design in [16]. It has a cylindrical volume of $\pi \times 21^2 \times 10$ mm^3 similar to the smartwatches available in the market such as Huawei Elegant ($\pi \times 22^2 \times 11.3$ mm^3). In our studies, the top and bottom circular surfaces are made from the Rogers substrates 4050B, with a thickness of 0.8 mm, a relative permittivity of 3.48, and a loss tangent of 0.0037. An annular slot, with a width of $W_s = 1$ mm, is cut along the edge on the top surface of the metallic cavity, as shown in Fig. 1(a). The circumference of the annular slot is $\pi\ (R_1 + R_2) = 122.5$ mm, about 1λ at 2.45 GHz. A shorting strip with a width of $W_1 = 1.7$ mm across the slot, as shown in Fig. 1(a), is used to short the inner portion of the slot to the system ground. A 50-Ω microstip feed line printed on the other side layer of the substrate, as shown in Fig.1(a) and (b), is used to coupled-feed the slot antenna. The microstrip feed line is directly connected to the metallic rim. Simulated results show that decreasing H or increasing W_s will shift the resonance to higher frequencies.

Simulation studies have shown that the angle θ between the microstrip feed line and shorting strip, as shown in Fig. 1(a), has significant effect on and in fact determines the resonances of the antenna. Fig. 2 shows the simulated S_{11} with the different values of θ (between 0° and 180°). It can be seen that the first-resonant frequency (i.e., the fundamental frequency) of the antenna increases with increasing θ. At $\theta = 10°$, as shown in Fig. 2(a), the antenna has a very weak first resonance at 2.42 GHz and a second resonance at

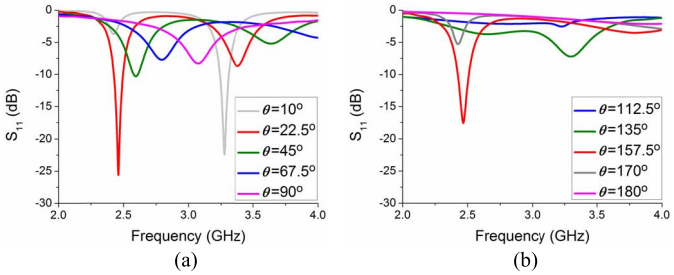

Fig. 2. Simulated S_{11} of antenna with different θ values. (a) $10° \le \theta \le 90°$. (b) $112.5° \le \theta \le 180°$.

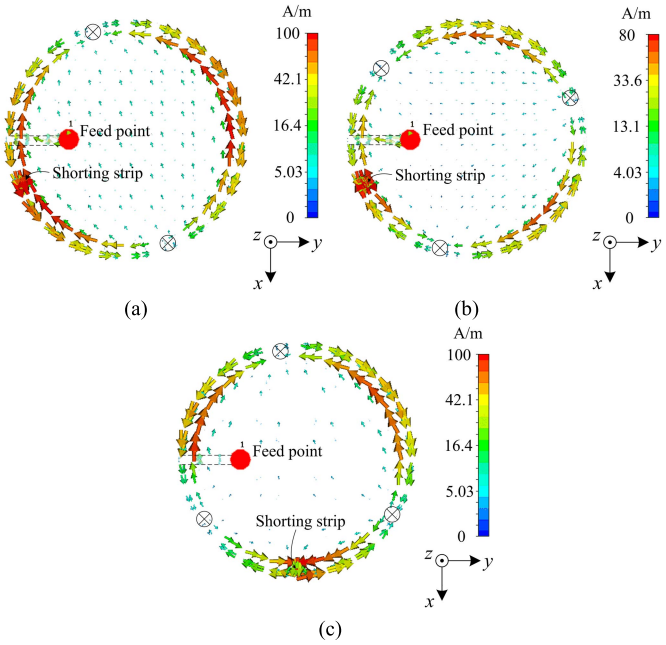

Fig. 3. Simulated surface current distribution. (a) $\theta = 22.5°$ at 2.45 GHz. (b) $\theta = 22.5°$ at 3.4 GHz. (c) $\theta = 90°$ at 3.08 GHz (⊗: current null).

3.3 GHz. With θ increased to 22.5°, the antenna generates a strong first resonance at 2.45 GHz and a second resonance at 3.4 GHz. As θ increases further to 45°, 67.5°, and 90°, the first resonance shifts to 2.6, 2.8, and 3.08 GHz, respectively, and becomes slightly weaker. In fact, the first resonance at $\theta = 90°$ was also found and studied in [19], but our results show that first resonances at lower frequencies can be generated using smaller θ. The lowest and also strongest first resonance obtained is at 2.45 GHz with $\theta = 22.5°$. Fig. 2(b) shows that, with θ further increases to 112.5° and 135°, the first resonance is still relatively weak at 2.83 and 2.65 GHz. However, when $\theta = 157.5°$, the first resonance suddenly becomes very strong at 2.45 GHz, similar to the one at $\theta = 22.5°$. At $\theta = 170°$, first resonance becomes weak again at 2.43 GHz. There is no resonance at $\theta = 180°$ in the frequency range tested.

Vector-current distributions of the antenna at different resonances have been used to further study the antenna operation. Fig. 3(a) shows the vector-current distribution of the antenna at the first-resonant frequency of 2.45 GHz, i.e., with $\theta = 22.5°$. It can be seen that there are two current nulls on the annular slot, indicating that the antenna is operating in the 1-λ mode. At the second-resonant frequency of 3.4 GHz, the vector-current distribution of the antenna is shown in Fig. 3(b), indicating that there are three current nulls on the slot, which suggests that the antenna is operating in the 1.5-λ mode. For comparison, the vector-current distribution of the antenna with $\theta = 90°$ at 3.08 GHz (the first-resonance) studied in [19] is shown

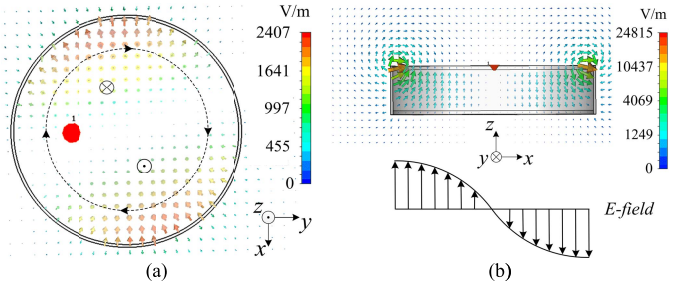

Fig. 4. Simulated E-field distribution in (a) xy plane and (b) xz plane at 2.45 GHz. ($\otimes$: E-field into xy plane and $\odot$: E-field out of xy plane).

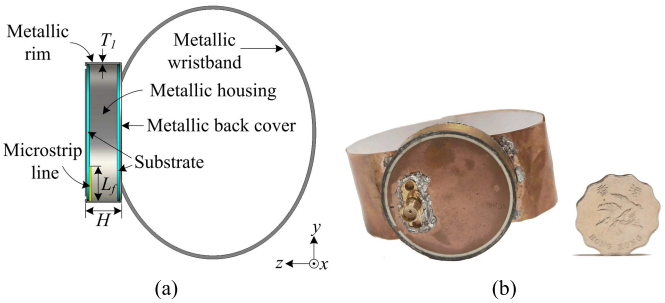

Fig. 5. Geometry of proposed smartwatch antenna (a) side view and (b) prototyped antenna.

TABLE II
DIMENSIONS OF SMARTWATCH (mm)

R_1	R_2	R	W_1	W_s
19	20	21	1.7	1
L_f	W_f	H	θ	T_1
10.5	1.74	10	22.5°	0.5

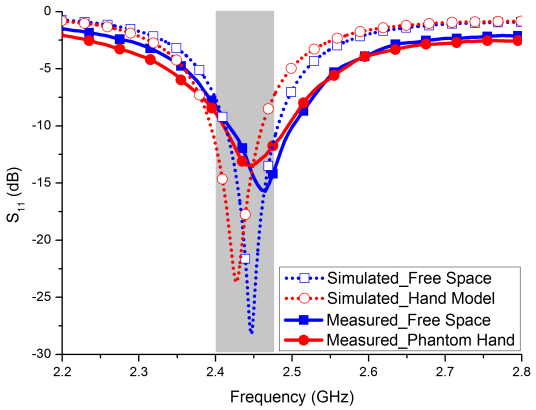

Fig. 6. Simulated and measured S_{11} of proposed antenna in free space, on the hand model, and on phantom hand.

in Fig. 3(c). It can be seen that there are three current nulls on the slot, confirming that the antenna at the first-resonance is operating in the 1.5-λ mode. This mode requires a circumference of 1.5λ for the annual slot, which at 2.45 GHz is too long for use in current smartwatches. However, with the use of $\theta = 22.5°$ and the 1-λ mode, the annular slot has a circumference of only about 1λ, which is small enough for current smartwatches.

To study the transverse mode, TM_{nml}, of the cavity antenna with $\theta = 22.5°$ in the 1-λ mode at 2.45 GHz, we investigate the E-field distributions in three transverse planes, the xy, xz, and yz planes, with the simulated results shown in Fig. 4. It can be seen in Fig. 4(a) that, along the perimeter of the circle as indicated in the xy plane, there is one wavelength variation of E-field, so $n = 1$. Fig. 4(b) shows that the E-field in the xz plane have a length of $\lambda/2$ and along the height H is constant, indicating that $m = 1$ and $l = 0$. The E-field distribution in the yz plane is similar to that in the xz plane and so is not shown here. Thus, the cavity antenna is operating in the TM_{110} mode.

Fig. 4(b) shows that the maximum E-field in the xz plane is 24 815 V/m (12 692 V/m in the yz plane), on the slot, as shown by the color bars. However, the maximum E-field inside the cavity is relatively weak at 2407 V/m, as shown in Fig. 4(a), which is about 9.7% of the maximum field on the annular slot. That means only a very small amount energy is stored inside the cavity, so metallic-electronic components placed inside the cavity (i.e., inside the smartwatch) will not affect the antenna performance much (as will be studied later).

III. Antenna Design and Discussion for Smartwatch

The cavity-backed annular slot antenna in Fig. 1 is proposed for the design of smartwatch antenna, as shown in Fig. 5. The top circular surface is for the smartwatch screen. The wristband is metallic, having a length of 180 mm and a width of 30 mm, and electrically connected to the metallic housing of the cavity, as shown in Fig. 5(a). Note that, the metallic wristband can also be made of nonmetallic materials, such as plastic and leather, which has little effect on the antenna performance. The dimensions of the proposed smartwatch antenna are listed in Table II and the prototype is shown in Fig. 5(b).

Unlike mobile phones or tablets, smartwatches are always worn on human hand, so it is more realistic to study the antenna performance using a computer hand model and a phantom hand. Here, the hand model used in our studies is the same as the one used in our previous work [16]. The hand model is in direct contact with the metallic wristband of the smartwatch without any gap. In the measurements, the phantom hand, Model IXB-053 from IndexSAR [22], is used for studies.

The simulated and measured S_{11} of the smartwatch antenna in free space, on the computer hand model, and on the phantom hand is shown in Fig. 6. It can be seen that the measured resonances are only slightly (less than 1%) higher than the corresponding simulated resonances, indicating good agreements. When an antenna is placed on a hand, the antenna resonance will normally shift at lower frequency due to larger ε_r of body issue. Fig. 6 shows that the simulated resonance shifts from 2.45 to 2.43 GHz when the smartwatch is on the computer hand model, and the measured resonance shifts from 2.47 to 2.45 GHz when the smartwatch is on the phantom hand. Both frequency shifts are quite small, less than 1%. However, among the designs in [7]–[15], the design in [12] had the least simulated and measured frequency shifts of about 8%, much large than 1% in our proposed antenna. The measured impedance bandwidths (IMBWs), for $S_{11} \leq -6$ dB, of the smartwatch antenna in free space and on the phantom hand are 2.38–2.54 GHz and 2.36–2.54 GHz, respectively, which are wide enough for the 2.4-GHz Wi-Fi/Bluetooth systems. Note that, $S_{11} \leq -6$ dB is used here to define the bandwidth, which is normally used in mobile antenna design in industry [23], and the simulated and measured S_{11} in the 2.4-GHz Wi-Fi/Bluetooth band in both free space and phantom hand are all less than -7.31 dB.

The simulated and measured efficiencies and realized peak gains of the antenna in free space, on the hand model, and on the phantom hand are shown in Fig. 7. A feeding cable is used in measurements but is not included in simulations. The efficiencies are the total

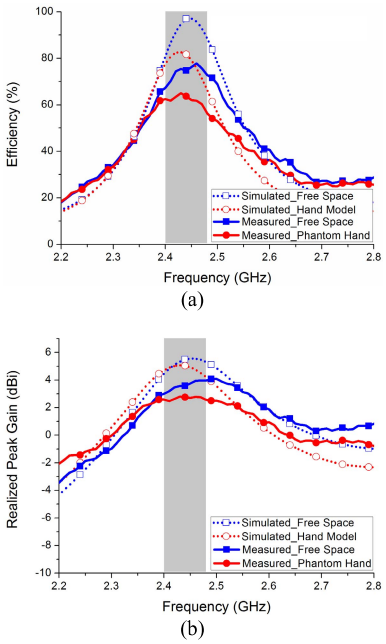

Fig. 7. Simulated and measured (a) efficiencies and (b) gains of proposed antenna in free space, on the hand model, and on phantom hand.

efficiencies which includes the loss due to antenna mismatching. The discrepancies between the simulated and measured results are due to the fabrication and measurement tolerances and mainly the feeding cable effects [24]. The simulated results in Fig. 7 do not include the feeding cable effects. The measured efficiencies are 70%–78% in free space and 57%–66% on the phantom hand in the 2.4-GHz Bluetooth/Wi-Fi band. The measured realized peak gains are 3–4 dBi in free space and 2.47–2.79 dBi on the phantom hand. The reason why the efficiencies and gains of the antenna on the phantom hand are higher than others is that, radiation in the $-z$-direction is smaller than that in the $+z$-direction, as shown in Fig. 8(a), and hence the EM energy absorbed by the phantom hand (in the $-z$-direction) is relatively smaller than those of antennas with omnidirectional radiation.

The simulated and measured radiation patterns of the antenna at 2.45 GHz are shown in Fig. 8. In free space, Fig. 8(a) shows that both the simulated and measured radiation patterns in the xz and yz planes of the antenna are nearly omnidirectional. The measured front-to-back ratio (FBR) computed using the total E-field is only 5.95 dB. The radiation pattern in the xy plane is also nearly omnidirectional radiation which is preferable for wireless devices. When the smartwatch is on the hand model for simulations or on the phantom hand for measurements, the radiation patterns in the xz and yz planes are shown in Fig. 8(b). It can be seen that the measured FBR substantially increases from 5.95 to 13.66 dB, which is due to radiation toward the $-z$-direction absorbed by the hand.

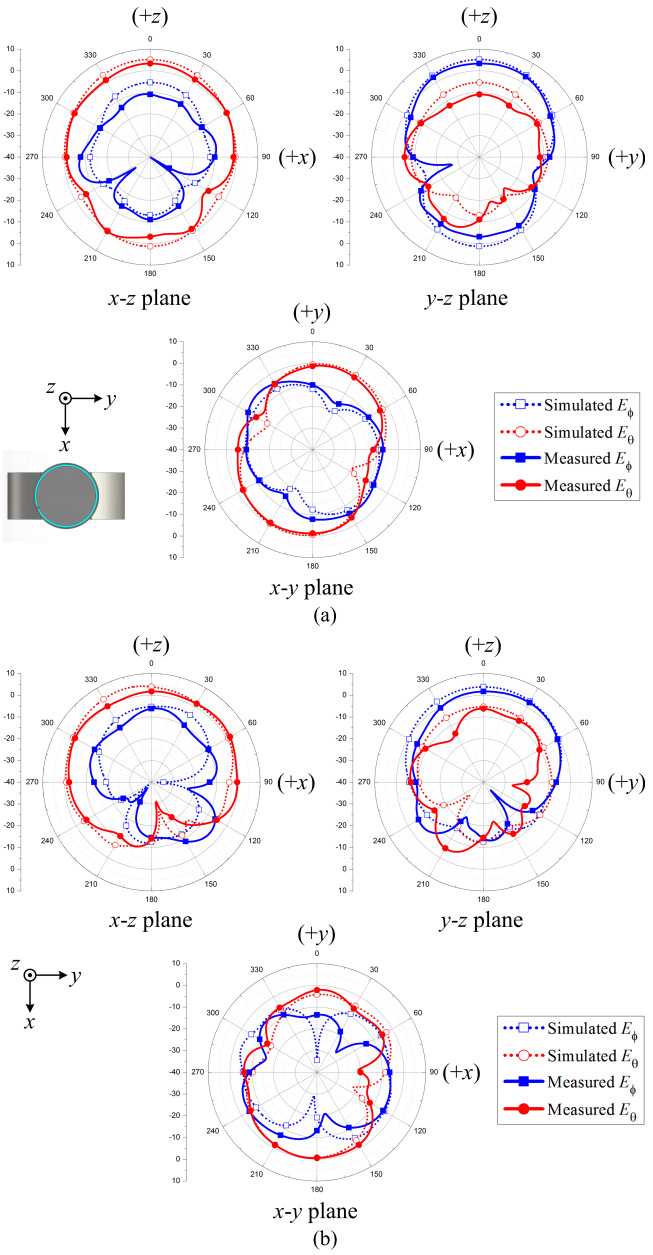

Fig. 8. Simulated and measured radiation patterns (a) in free space and (b) on the hand model and phantom hand.

IV. Effects of Electronic Components Inside Metallic Cavity

In practice, there will be electronic components, such as integrated chips, sensors, and batteries on the printed circuit board inside the smartwatch. To make our simulation model more realistic, we place a metallic block which has a cylindrical shape with a volume of $\pi \times 19^2 \times 6$ mm^3 inside the cavity of the smartwatch, as shown in Fig. 9, to simulate the electronic components inside the smartwatch. The simulated S_{11} of the antenna with and without the metallic block are shown in Fig. 10(a). It can be seen that putting the metallic block inside the cavity shifts the resonant frequency from 2.45 to 2.84 GHz. To operate in the Wi-Fi/Bluetooth band, the resonant frequency needs to be shifted back to 2.45 GHz. As mentioned earlier, increasing the cavity depth H or decreasing the width W_s can shift the resonant frequency to lower frequencies. Since H relates to the thickness of the smartwatch and is often fixed in a design, we propose to decrease the slot width W_s to shift the resonant frequency back to 2.45 GHz. Simulation studies have shown that, with W_s decreased from 1 to 0.42 mm, the resonant frequency shifts back to 2.45 GHz, as shown in Fig. 10(a). Although the IMBW also reduces slightly to 2.4–2.48 GHz, it can cover the 2.4-GHz Bluetooth/Wi-Fi systems. The simulated efficiencies of the antenna, with and without the metallic block and with W_s reduced to 0.42 mm, are shown in Fig. 10(b). It can be seen that, with $W_s = 0.42$ mm, the efficiency at the

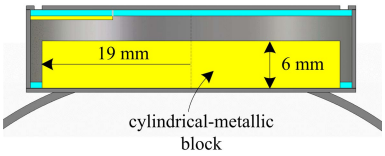

Fig. 9. Simulated model of smartwatch with metallic block inside.

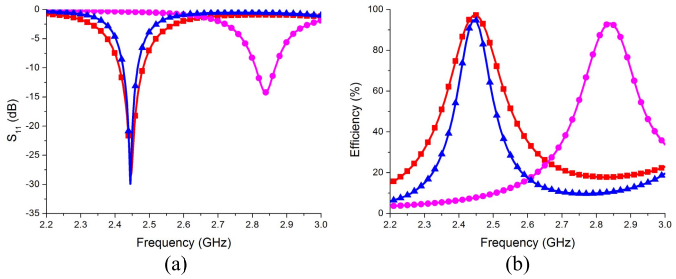

Fig. 10. Simulated (a) S_{11} and (b) efficiencies of proposed antenna with and without metallic block. [Red line: without metallic block (WS = 1 mm), pink line: with metallic block (WS = 1 mm), and blue line: with metallic block (WS = 0.42 mm)].

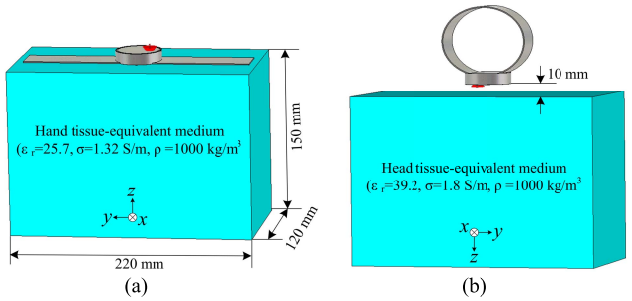

Fig. 11. SAR simulation models for (a) wrist-worn and (b) next-to-mouth conditions.

center frequency of 2.45 GHz is not changed much and in the IMBW of 2.4–2.48 GHz is within 64%–95%. Hence, putting metallic components inside the smartwatch does not alter much the antenna performance, except the resonant frequency.

V. SAR Analysis

The SAR is a value set to limit EM radiated power from wireless devices and absorbed by users. It represents the RF power-absorption rate by a certain mass of tissue and is given by [25]

$$\text{SAR} = \frac{\sigma |E|^2}{\rho} \tag{1}$$

where σ and ρ are the conductivity (S/m) and mass density (kg/m^3), respectively, of the tissue considered, and E is the root-mean-square value of electric field strength (V/m) in the tissue.

According to the regulations set by the Federal Communication Commission (FCC), the SARs of wrist-worn wireless devices should be evaluated in two conditions with the device: 1) worn on the wrist and 2) positioned next to the mouth while the device is operating in the speaker mode for voice communication [26]. To measure the SAR values in these conditions, the FCC requires using a flat phantom filled with hand and head tissue-equivalent medium [26]. In the worn-on-wrist condition, the back of the smartwatch should be positioned in direct contact with the flat phantom without any gap as shown in Fig. 11(a). In the next-to-mouth condition, the front of the smartwatch should be positioned at 10 mm from the flat phantom.

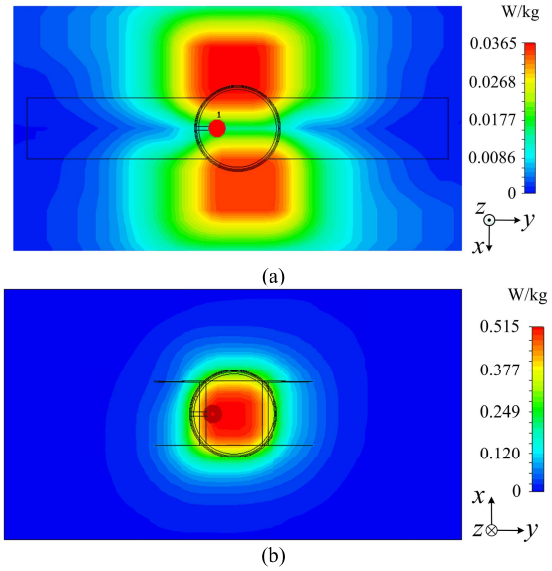

Fig. 12. Top view: SAR distribution. (a) 10-g SAR for wrist-worn condition. (b) 1-g SAR for next-to-mouth condition.

Regarding the phantom shape, as recommended in IEEE Std 1528-2013 [25], the flat phantom for SAR evaluation should be rectangular with a dimension of 220 mm$^3\times$ 120 mm$^3\times$ 150 mm^3. Human tissue is lossy and the different parts of human body have different relative (ε_r) and conductivities (σ) which vary with frequency. According to IEEE Std 1528-2013 [25], at the operating frequency of 2.45 GHz, the hand tissue-equivalent medium has $\varepsilon_r = 25.7$ and $\sigma = 1.32$ S/m and the head tissue-equivalent medium has $\varepsilon_r = 39.2$ and $\sigma = 1.8$ S/m. The mass densities (ρ) of the hand and head tissue-equivalent media are 1000 kg/m^3 [27]. With all these requirements, we develop the phantom models, as shown in Fig.11(a) and (b) in CST, for evaluation of SAR in the worn-on-wrist and next-to-mouth conditions, respectively. In our studies, we set the input power to the smartwatch antenna to 18.5 dBm for Wi-Fi applications, which is based on the value used in the MediaTek MT2502 platform for wearables and IoT devices [28].

Fig. 12 shows the simulated SAR distributions at 2.45 GHz in the wrist-worn and next-to-mouth conditions. In the wrist-worn condition, Fig. 12(a) shows that, the SAR distribution is mainly concentrated in the $+x$ and $-x$ sides of the smartwatch. This is due to the locations of the two current nulls [on the annular slot, as shown in Fig. 3(a)] which have the maximum voltage, and, hence the maximum E-field. The 10-g SAR value is about 0.036 W/kg. For the next-to-mouth condition, Fig. 12(b) shows that the SAR distribution is quite uniform on the area around the smartwatch. The 1-g SAR value is about 0.515 W/kg. Both SAR values are less than the corresponding SAR limitations of 4 W/kg and 1.6 W/kg, set by the FCC [26].

VI. Conclusion

A cylindrical cavity-backed annular slot antenna for smartwatch applications with high efficiency has been proposed. The cavity has an annular slot cut along the edge of the top surface. The resonant modes of the antenna have been studied using simulations. Results have shown that using an angle of 22.5° between the microstrip feed line and shorting strip on the annular slot, the antenna can generate a 1-λ mode, resulting in a compact cavity size suitable for current smartwatches. The smartwatch has been studied in free space, on a computer hand model, and on a phantom hand using simulations and measurements. Measured results have shown that when worn on the

phantom hand, the antenna has an efficiency of 57%–66% in the 2.4-GHz Bluetooth/Wi-Fi band, much higher than the other designs. More studies have shown that electronic components placed inside the cavity have little effect on the antenna performance and the SAR values of the antenna can satisfy the SAR limitations set by the FCC.

REFERENCES

[1] *Wearable Antennas, Antenna Theory*, accessed on Oct. 12, 2016. [Online]. Available: http://www.antenna-theory.com/antennas/wearable-antennas.php

[2] *LVL—Wearable Hydration Monitor*, accessed on Oct. 12, 2016. [Online]. Available: http://www.onelvl.com/

[3] *Halowearables*, accessed on Oct. 12, 2016. [Online]. Available: https://halowearables.com/

[4] Wikipedia. *Wearable Technology*, accessed on Oct. 12, 2016. [Online]. Available: https://en.wikipedia.org/wiki/Wearable_technology

[5] Qualcomm Inc., San Diego, CA, USA. *Wearables*, accessed on Oct. 12, 2016. [Online]. Available: https://www.qualcomm.com/solutions/internet-of-things/consumer-electronics/wearables

[6] TE Connectivity Ltd, Schaffhausen, Switzerland. *Antenna Technologies for Wearables*, accessed on Oct. 12, 2016. [Online]. Available: http://www.te.com/usa-en/industries/consumer-solutions/insights/antenna-technologies-for-wearables.html

[7] K. Zhao, S. Zhang, C.-Y. Chiu, Z. Ying, and S. He, "SAR study for smart watch applications," in *Proc. IEEE Antennas Propag. Soc. Int. Symp. (APSURSI)*, Memphis, TN, USA, 2014, pp. 1198–1199.

[8] H. Hamouda, P. Le Thuc, R. Staraj, and G. Kossiavas, "Small antenna embedded in a wrist-watch for application in telemedicine," in *Proc. 8th Eur. Conf. Antennas Propag. (EuCAP)*, Hague, The Netherlands, Apr. 2014, pp. 876–879.

[9] C.-H. Wu, K.-L. Wong, Y.-C. Lin, and S.-W. Su, "Internal shorted monopole antenna for the watch-type wireless communication device for bluetooth operation," *Microw. Opt. Technol. Lett.*, vol. 49, pp. 942–946, Apr. 2007.

[10] K. Zhao, Z. N. Ying, and S. L. He, "Antenna designs of smart watch for cellular communications by using metal belt," in *Proc. 9th Eur. Conf. Antennas Propag. (EuCAP)*, Lisbon, Portugal, 2015, pp. 1–5.

[11] S. Sojuyigbe and K. Daniel, "Wearables/IOT devices: Challenges and solutions to integration of miniature antennas in close proximity to the human body," in *Proc. IEEE Symp. Electromagn. Compat. Signal Integrity*, Santa Clara, CA, USA, Mar. 2015, pp. 75–78.

[12] S.-W. Su and Y.-T. Hsieh, "Integrated metal-frame antenna for smartwatch wearable device," *IEEE Trans. Antennas Propag.*, vol. 63, no. 7, pp. 3301–3305, Jul. 2015.

[13] M. Jeon, W. C. Choi, and Y. J. Yoon, "GPS, Bluetooth and Wi-Fi tri-band antenna on metal frame of smartwatch," in *Proc. IEEE Int. Symp. Antennas Propag. (APSURSI)*, Fajardo, Puerto Rico, Jun. 2016, pp. 2177–2178.

[14] L.-J. Xu and Z. Duan, "Differential wide band metal-frame antenna for wristband applications," in *Proc. IEEE MTT-S Int. Microw. Workshop Ser. Adv. Mater. Processes RF THz Appl. (IMWS-AMP)*, Chengdu, China, Jul. 2016, pp. 1–3.

[15] "2.4 GHz: Weii ceramic antenna," Tech. Specification SRCW004, Antenova Ltd., Hatfield, U.K., 2015.

[16] D. Wu, S. W. Cheung, Q. L. Li, and T. I. Yuk, "Slot antenna for all-metal smartwatch applications," in *Proc. 10th Eur. Conf. Antennas Propag. (EuCAP)*, Davos, Switzerland, Apr. 2016, pp. 1–4.

[17] J. Galejs and T. Thompson, "Admittance of a cavity-backed annular slot antenna," *IRE Trans. Antennas Propag.*, vol. 10, no. 6, pp. 671–678, Nov. 1962.

[18] N. Nikolic, J. S. Kot, and T. S. Bird, "Theoretical and experimental study of a cavity-backed annular-slot antenna," *IEE Proc. Microw., Antennas Propag.*, vol. 144, no. 5, pp. 337–340, Oct. 1997.

[19] H. Morishita, K. Hirasawa, and K. Fujimoto, "Analysis of a cavity-backed annular slot antenna with one point shorted," *IEEE Trans. Antennas Propag.*, vol. 39, no. 10, pp. 1472–1478, Oct. 1991.

[20] *SATIMO*. [Online]. Available: http://www.satimo.com

[21] *Test Plan for Mobile Station Over-the-Air Performance, Rev. 3.4*, CTIA, Washington, DC, USA, Dec. 2014.

[22] IndexSAR. [Online]. Available: http://indexsar.com

[23] K. L. Wong, *Planar Antennas for Wireless Communications*. New York, NY, USA: Wiley, 2003.

[24] L. Liu, S. W. Cheung, Y. F. Weng, and T. I. Yuk, "Cable effects on measuring small planar UWB monopole antennas," in *Ultra Wideband*, M. A. Matin, Ed. Rijeka, Croatia: InTech, Oct. 2012.

[25] *IEEE Recommended Practice for Determining the Peak Spatial-Average Specific Absorption Rate (SAR) in the Human Head from Wireless Communications Devices: Measurement Techniques*, IEEE Standard 1528, 2013.

[26] *447498 D01 General RF Exposure Guidance v06, RF Exposure Procedures and Equipment Authorization Policies for Mobile and Portable Devices*, Federal Commun. Commission Office Eng. Technol. Lab. Division, Washington, DC, USA, Oct. 2015.

[27] S. P. Singh and P. Mehta, *Human Body Measurements: Concepts and Applications*. New Delhi, India: PHI Learning Private Limited, 2009.

[28] *MT2502 Chipset Technical Brief*, MediaTek Ltd., Hsinchu, Taiwan 2014.